

Contribution from the Fachbereich Chemie, Universität Dortmund, 4600 Dortmund, FRG, and Sektion für Röntgen- und Elektronenbeugung, Universität Ulm, 7900 Ulm, FRG

cis- $[(\text{NH}_3)_2\text{Pt}(\text{1-MeU})_2\text{Pt}(\text{bpy})]_2(\text{NO}_3)_5 \cdot m\text{HNO}_3 \cdot n\text{H}_2\text{O}$, a Pt(2.25) Blue Derived from a Dinuclear, Mixed-Amine Complex of 1-Methyluracil (1-MeUH). Characterization of the Cation, Analytical Evaluation of Cocrystallized HNO_3 , and X-ray Structure of Its Reduced $[\text{Pt}^{2.0}]_2$ Form

Gabriele Trötscher,^{1a} Wolfgang Micklitz,^{1a,b} Helmut Schöllhorn,^{1c} Ulf Thewalt,^{1c} and Bernhard Lippert^{*1a}

Received May 12, 1989

Several samples of tetranuclear Pt(2.25) complexes **2** derived from the mixed-amine complex *cis*- $[(\text{NH}_3)_2\text{Pt}(\text{1-MeU})_2\text{Pt}(\text{bpy})](\text{NO}_3)_2 \cdot 3\text{H}_2\text{O}$ (**1**) (1-MeU = 1-methyluracil anion, $\text{C}_5\text{H}_5\text{N}_2\text{O}_2$, bpy = 2,2'-bipyridine) upon chemical (Ce(IV), HNO_3) oxidation in acidic medium have been isolated and studied by elemental analysis, potentiometric titration, and visible spectroscopy. All samples of **2** contained variable amounts of HNO_3 incorporated in the crystals, ranging from 0.3 to 4.7 equiv per $[\text{Pt}^{2.25}]_4$, as demonstrated by titration with NaOH and elemental analysis. The features of the NaOH titration curves of **2** not only depend on the amount of HNO_3 present in the respective sample but also display a strong time dependence. This is explained by several consecutive processes, which include (i) a disproportionation of **2** into $[\text{Pt}^{\text{III}}]_2$ and $[\text{Pt}^{\text{II}}]_2$ (**1**) species, (ii) water oxidation by $[\text{Pt}^{\text{III}}]_2$ and generation of H^+ , and (iii) partial dissociation of $[\text{Pt}^{\text{II}}]_2$ (**1**). The spontaneous reduction of **2** in water (acidic pH) is unambiguously demonstrated by the isolation of **1***, which proved to be identical with **1**. A disproportionation, although chemically feasible, has not explicitly been demonstrated to be part of this process. In aqueous solution, **1** undergoes stacking via the bpy ligands, as shown by ^1H NMR spectroscopy. Crystal data for **1***: triclinic space group $P\bar{1}$, $a = 11.137$ (2) Å, $b = 11.953$ (2) Å, $c = 13.405$ (3) Å, $\alpha = 101.90$ (3)°, $\beta = 113.52$ (3)°, $\gamma = 101.73$ (3)°, $V = 1517.8$ Å³, $Z = 2$. The Pt-Pt separation within the dinuclear complex is 2.929 (1) Å.

Introduction

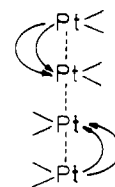
Structurally characterized "platinum blues" to date are restricted to four examples,² all of which comprise pairs of dinuclear Pt_2 complexes with identical amine ligands at the metals and two bridging ligands arranged head to head (Chart I). The average Pt oxidation state in these compounds is 2.25, resulting formally from the presence of Pt(II) and Pt(III) in a ratio of 3:1. Related to these "blues" are "tans",³ "greens",⁴ and "violets"⁵ of different average oxidation states yet with similar structural features.

Recently, a trinuclear, mixed-metal $\text{Pt}^{\text{II}}_2\text{Pd}^{\text{III}}$ complex has been added to the list of "blues" and was considered a model of a yet uncharacterized Pt(2.33) complex.⁶

All these compounds have in common the feature of identical amine ($(\text{NH}_3)_2$ or en) ligands at all Pt atoms. As has now been demonstrated,⁷ it is also possible to obtain "blues" in systems containing different amine groups coordinated to Pt. Pt(2.25) blues have been generated in solution through oxidative titration (Ce^{IV}) of dinuclear mixed-amine complexes of types $[(\text{en})\text{Pt}(\text{1-MeU})_2\text{Pt}(\text{NH}_3)_2]^{2+}$ and *cis*- $[(\text{NH}_3)_2\text{Pt}(\text{1-MeU})_2\text{Pt}(\text{bpy})]^{2+}$ with 1-MeU being the anionic 1-methyluracilato ligand, $\text{C}_5\text{H}_5\text{N}_2\text{O}_2^-$. In this paper, the synthesis and characterization of a Pt(2.25) blue derived from the mixed $(\text{NH}_3)_2/\text{bpy}$ complex is reported.

In the course of this work, a major problem concerning the proper characterization of all these compounds isolated from strongly acidic medium became evident: The differentiation of

Chart I



an anion, e.g. NO_3^- , from its conjugated acid HNO_3 , albeit dramatic in its effect on cation charge and hence metal oxidation state, is impossible by elemental analysis and frequently very difficult even with results from X-ray analysis available. A specific example refers to a blue derived from $[(\text{bpy})\text{Pt}(\text{1-MeU})_2\text{Pt}(\text{bpy})]^{2+}$ (head-head):⁸ Despite a reasonably well-refined cation (dimer-of-dimers structure) with Pt-Pt separations of 2.743 (3) Å (within dimers) and 2.868 (4) Å (between dimers), the location and differentiation of NO_3^- counterions, cocrystallized HNO_3 and water of crystallization represents a major problem. Pt-Pt separations, although of some help with regard to assigning metal oxidation states, are known to be too sensitive to effects imposed by ligand geometries to unambiguously permit conclusions. Even with counterions that are reasonably well refined, the problem of crystallographically differentiating between a H_3O_2^+ and two strongly H-bonded H_2O molecules may pose a problem: A dinuclear 1-methylcytosinato complex, previously described as a $[\text{Pt}^{2.5}]_2$ compound,⁹ actually is a $[\text{Pt}^{3.0}]_2$ compound and has been misinterpreted for this very reason.

Therefore, we have undertaken a study to analyze our mixed-amine blue in more detail and to pay particular attention to the question of cocrystallized acid.

In this study, we found evidence that the $[\text{Pt}^{2.25}]_4$ blue undergoes a spontaneous reduction when dissolved in water. The reduction product was analyzed by X-ray crystallography and proved to be the diplatinum(II) complex *cis*- $[(\text{NH}_3)_2\text{Pt}(\text{1-MeU})_2\text{Pt}(\text{bpy})](\text{NO}_3)_2 \cdot 3\text{H}_2\text{O}$.

Experimental Section

Preparation. Compounds of general formula $[(\text{NH}_3)_2\text{Pt}(\text{1-MeU})_2\text{Pt}(\text{bpy})]_2(\text{NO}_3)_5 \cdot m\text{HNO}_3 \cdot n\text{H}_2\text{O}$ (**2**) were prepared from a dinu-

- (1) (a) Universität Dortmund. (b) Present address: Department of Chemistry, MIT, Cambridge, MA 02139. (c) Universität Ulm.
- (2) (a) Barton, J. K.; Szalda, D. J.; Rabinowitz, H. N.; Waszczak, J. V.; Lippard, S. J. *J. Am. Chem. Soc.* **1979**, *101*, 1434. (b) Ginsberg, A. P.; O'Halloran, T. V.; Fanwick, P. E.; Hollis, L. S.; Lippard, S. J. *J. Am. Chem. Soc.* **1984**, *106*, 5430. (c) O'Halloran, T. V.; Mascharak, P. K.; Williams, I. D.; Roberts, M. M.; Lippard, S. J. *Inorg. Chem.* **1987**, *26*, 1261 and references cited therein. (d) Sakai, K.; Matsumoto, K. *J. Am. Chem. Soc.* **1989**, *111*, 3074.
- (3) (a) Matsumoto, K.; Fuwa, K. *J. Am. Chem. Soc.* **1982**, *104*, 897. (b) Matsumoto, K.; Takahashi, H.; Fuwa, K. *Inorg. Chem.* **1983**, *22*, 4086. (c) Matsumoto, K. *Chem. Lett.* **1984**, 2061.
- (4) Matsumoto, K.; Takahashi, H.; Fuwa, K. *J. Am. Chem. Soc.* **1984**, *106*, 2049.
- (5) Matsumoto, K. *Bull. Chem. Soc. Jpn.* **1985**, *58*, 651.
- (6) (a) Micklitz, W.; Müller, G.; Huber, B.; Riede, J.; Lippert, B. *J. Chem. Soc., Chem. Commun.* **1987**, 76. (b) Micklitz, W.; Müller, G.; Huber, B.; Riede, J.; Rashwan, F.; Heinze, J.; Lippert, B. *J. Am. Chem. Soc.* **1988**, *110*, 7084.
- (7) Micklitz, W.; Riede, J.; Huber, B.; Müller, G.; Lippert, B. *Inorg. Chem.* **1988**, *27*, 1979.

- (8) Micklitz, W.; Sheldrick, W. S.; Lippert, B. Unpublished results.
- (9) Faggiani, R.; Lippert, B.; Lock, C. J. L.; Speranzini, R. A. *J. Am. Chem. Soc.* **1981**, *103*, 1111.

Table I. Elemental Analyses of HNO₃-Containing Products of **2**, [(NH₃)₂Pt(1-MeU)₂Pt(bpy)](NO₃)₂·*m*HNO₃·*n*H₂O

compd	element	% found	ratio	<i>m</i>	<i>n</i>	% calcd
2a	C	19.98	40	4.6	6	20.28
	H	2.77	66.1			2.75
	N	14.90	25.6			15.14
	O	28.70	43			28.90
2a*	C	21.97	40	1.4	5	22.35
	H	2.78	60			2.78
	N	14.34	22.4			14.60
2b	C	22.34	40	2	3	22.33
	H	2.61	55.8			2.62
	N	14.99	23			14.98
	O	23.52	31.6			23.80

clear precursor, *cis*-[(NH₃)₂Pt(1-MeU)₂Pt(bpy)](NO₃)₂·3H₂O (**1**), which in turn was obtained by reaction of *cis*-(NH₃)₂Pt(1-MeU)₂·4H₂O¹⁰ with [Pt(bpy)(H₂O)₂](NO₃)₂ and subsequent recrystallization from H₂O/acetone.⁷ Oxidation of **1** was achieved via two routes.

(i) Addition of 3 mL of concentrated HNO₃ (14 N) to an aqueous suspension of **1** (100 mg of **1** suspended in 20 mL) resulted in a rapid color change from the original red to dark violet. It was found that the yield of **2** could be improved by using a minimum amount of water for suspension. With no water added, **2** is further oxidized either to a di-platinum(III) (yellow) or, with ligand cleavage, to a platinum(IV) species (yellow), however.

After filtration of some residue, crystallization of **2** took place rapidly at room temperature. For further crystallization, the solution was kept at 3 °C. Within 24 h, dark violet crystals of the title compound were recovered. They were washed twice with 0.5 mL of ice water and air-dried (1 day). The crystals had a strong smell of HNO₃, suggesting that HNO₃ is lost during storage. Depending on the amount of HNO₃ used (e.g. 5–10 mL) and time of crystallization (1 day, 10 days) products with different HNO₃ contents were obtained. Yields were generally variable (12–50%). Table I gives the results for two representative samples (**2a**, **2b**) and for a third one (**2a***) obtained from **2a** by storage over NaOH for 12 h and subsequent storage under vacuum (1 day). In all samples, the C:N ratio was taken as an indication of the amount of HNO₃ present with the tetranuclear structure assumed. If crystals of **2** were not removed from solution after 24 h but rather kept in it for 10 days or longer and then filtered off (**2c**), they had a somewhat different habit (lustrous green; black-purple when crushed) and an EPR spectrum that was slightly different from that of **2a** (cf. supplementary material). The yield of **2c** was 50%. The sample analyzed for *m* = 1, *n* = 5.

(ii) In an alternative method, **1** (120 mg) was suspended in 0.14 N HNO₃ (5 mL), and Ce(SO₄)₂·4H₂O (48 mg, 1 equiv/dimer) was added. The blue-purple solution was filtered from some undissolved residue and allowed to slowly evaporate (2 days at 3 °C). Blue-purple crystals were then filtered off, washed four times with ice water (0.5 mL) and dried in air (1 day). Yields were quite unpredictable, ranging from 6% to 30%. Samples of five different preparations (**2d**) showed that, within the accuracy of the elemental analysis, the crystals were free of HNO₃, and had a content of water of crystallization of 10 ± 1. An example follows. Anal. Found: C, 22.35; H, 2.80; N, 13.63 (C:H:N = 40:60:21). Calcd for the nonhydrate: C, 22.51; H, 3.11; N, 13.78. On the basis of the results of the potentiometric titrations with NaOH (cf. Results and Discussion), the presence of 0.3–0.4 equiv of HNO₃/[Pt²⁺]₄ was estimated. This amount of HNO₃ is well within the limits of N determination (±0.3%).

Crystals of the sample that was studied by X-ray crystallography were obtained in the following manner: 10 mg of **2** was dissolved in 10 mL of H₂O, and NaNO₃ was added. The purple solution of pH 4 was kept in a stoppered vessel at 40 °C for 1 week and allowed to crystallize at 3 °C. The red crystals then isolated (**1***) proved to be identical with the starting material **1** (IR, elemental analysis, cell constants).

Solution Studies. UV-vis spectra were recorded on a Perkin-Elmer 555 instrument. The oxidation studies were carried out in 1 N H₂SO₄ in a thermostated vessel at 25 °C with Ce(SO₄)₂·4H₂O (dissolved in 1 N H₂SO₄) being the oxidizing agent. Typically, the concentrations of the complex to be oxidized were 1 × 10⁻³ M while that of Ce(IV) ranged from 1.3 × 10⁻² to 1.3 × 10⁻¹ M. The Pt combination electrode (Metrohm, Ag/AgCl reference) used to monitor the redox reactions was standardized in a saturated solution of chinhydrone in pH 4 buffer (*E* = 259 ± 5 mV). For spectrophotometrically monitored oxidations, samples were removed from the reaction vessel, measured in 2-mm cells, and returned to the reaction mixture afterward. Respective voltages were

Table II. Crystallographic Data for *cis*-[(NH₃)₂Pt(1-MeU)₂Pt(bpy)](NO₃)₂·3H₂O (**1***)

fw	1008.68	<i>d</i> _{calcd} , g cm ⁻³	2.207
space group	P $\bar{1}$	<i>d</i> _{meas} , g cm ⁻³	2.216
<i>a</i> , Å	11.137 (2)	cryst size, mm	0.05, 0.1, 0.1
<i>b</i> , Å	11.953 (2)	μ , cm ⁻¹	45
<i>c</i> , Å	13.405 (3)	θ _{range} , deg	2–25
α , deg	101.90 (3)	no. of unique reflns	5271
β , deg	113.52 (3)	no. of reflns used in the calcs	4633 (<i>F</i> ₀ > 2 σ (<i>F</i> ₀))
γ , deg	101.73 (3)	<i>R</i> (<i>F</i>)	0.051
<i>V</i> , Å ³	1517.8	<i>R</i> _w (<i>F</i>) ^a	0.052
<i>Z</i>	2		

$$^a w^{-1} = \sigma^2(F) + 0.0012F^2.$$

taken when a constant value was reached. Stability measurements of **2** in solution were followed by UV-vis spectrophotometry in 2-mm cells with the corresponding solvent as reference. As solvents were used pure water, 0.14 N HNO₃ and 1.4 N HNO₃. The concentrations of the investigated solutions were typically 1.5 × 10⁻⁴ to 1.5 × 10⁻⁵ M.

¹H NMR spectra were recorded on a 300-MHz Bruker AM 300 instrument (D₂O, TSP as internal reference).

Other Measurements. Titrations with 0.2 N NaOH were carried out in an atmosphere of N₂ with samples of **2** (6–17 mg) dissolved in 10 mL of water. Changes in pH were monitored by use of a combination glass electrode and a pH meter (Metrohm) or by use of an automated titroprocessor (Model 686, Metrohm).

The magnetic moment of a HNO₃-containing sample of **2** was measured in the solid state at room temperature by using a magnetic balance (Johnson Matthey). The EPR spectra of two different, HNO₃-containing samples (**2a**, **2c**) were obtained at room temperature on a Varian E3 spectrometer at 9.175–9.177 GHz. Diphenylpicrylhydrazyl (DPPH) was used as an external standard.

Crystallography. The X-ray data were collected at room temperature on a Philips PW-1100 single-crystal diffractometer by using graphite-monochromated Mo K α radiation (λ = 0.71069 Å). The unit cell dimensions were calculated from 28 reflections. Crystal and structure determination data are summarized in Table II. *Lp* and, in a later stage, empirical absorption¹¹ corrections were applied. The positions of the Pt atoms were obtained from a three-dimensional Patterson map. Subsequent ΔF syntheses provided the positions of the non-hydrogen atoms. Hydrogens were ignored. All atoms were refined with anisotropic thermal parameters. Final atomic coordinates are given in Table III. The anisotropic thermal parameters are included in the supplementary material. The highest peak in the final difference map was 1.52 e Å⁻³ (1.1 Å away from Pt1). Complex scattering factors for neutral atoms were taken from ref 12. For calculations, the SHELX program package was used.¹³

Results and Discussion

Characterization of **2.** As previously reported,⁷ oxidation of *cis*-[(NH₃)₂Pt(1-MeU)₂Pt(bpy)]²⁺ by means of Ce(IV) in H₂SO₄-acidified solution led to a sharp increase in potential after addition of 0.25 equiv of Ce(IV)/Pt(II), suggesting the formation of a Pt(2.25) species (*E*⁰ = 703 mV vs Ag/AgCl). The visible spectrum of the solution at this point is virtually identical with that of the isolated complex **2** (vide infra). In a second process, the Pt(2.25) species is further oxidized (*E*⁰ = 933 mV vs Ag/AgCl), mainly to an orange-yellow diplatinum(III) complex with consumption of an additional 0.75 equiv or more of Ce(IV) and loss of the characteristic blue-purple color of **2**. We tentatively attribute the somewhat variable Ce(IV) consumption (0.75–0.83 equiv) to partial dissociation of the dimer unit and partial oxidation to Pt(IV). Likewise, isolated **2**, when redissolved in 0.72–1 N H₂SO₄, was oxidized by Ce(IV) in a similar fashion, again with a somewhat higher consumption of Ce(IV) (0.84–0.93 equiv) than anticipated. Solid samples of **2a**, **2b**, and **2d** had a very similar appearance immediately after isolation, displaying an intense blue-violet metallic luster. Upon storage, HNO₃-containing crystals occasionally adopted a metallic green luster with time.

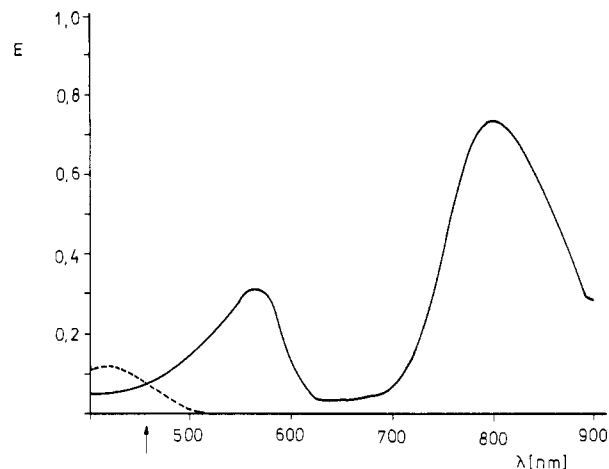
- (11) Walker, N.; Stuart, D. *Acta Crystallogr., Sect. A: Found. Crystallogr.* **1983**, *A39*, 158.
- (12) (a) Cromer, D. T.; Mann, J. B. *Acta Crystallogr., Sect. A: Cryst. Phys., Diffraction, Theor. Gen. Crystallogr.* **1968**, *A24*, 321. (b) Cromer, D.; Liberman, D. *J. Chem. Phys.* **1970**, *53*, 1891.
- (13) Sheldrick, G. M. *SHELX, Program for Crystal Structure Determination*; University of Göttingen: Göttingen, West Germany, 1976.

Table III. Atomic Coordinates and Equivalent Isotropic Temperature Factors (\AA^2) for **1***

atom	x	y	z	U
Pt1	0.0954 (1)	0.4664 (1)	0.1226 (1)	0.035 (1)
Pt2	0.2873 (1)	0.4754 (1)	0.3523 (1)	0.028 (1)
N10	0.1978 (10)	0.4598 (9)	0.0290 (8)	0.035 (4)
N11	0.0108 (11)	0.2925 (10)	0.0313 (9)	0.043 (5)
C10	0.2907 (14)	0.5541 (7)	0.0344 (14)	0.062 (8)
C11	0.3498 (16)	0.5432 (19)	-0.0384 (16)	0.069 (10)
C12	0.3172 (15)	0.4358 (19)	-0.1135 (13)	0.063 (8)
C13	0.2208 (17)	0.3318 (18)	-0.1216 (13)	0.067 (9)
C14	0.1613 (14)	0.3503 (15)	-0.0454 (11)	0.051 (7)
C15	0.0591 (13)	0.2556 (13)	-0.0428 (12)	0.048 (16)
C16	0.0102 (17)	0.1349 (14)	-0.1107 (13)	0.058 (7)
C17	-0.0936 (20)	0.0527 (17)	-0.1024 (15)	0.080 (9)
C18	-0.1459 (18)	0.0936 (15)	-0.0308 (15)	0.065 (8)
C19	-0.0938 (16)	0.2146 (14)	0.0350 (13)	0.058 (7)
N20	0.2839 (11)	0.2982 (9)	0.3177 (10)	0.046 (5)
N21	0.4710 (10)	0.5203 (10)	0.3426 (9)	0.041 (5)
N1a	0.3838 (10)	0.8427 (9)	0.5338 (9)	0.039 (5)
C1a'	0.4605 (17)	0.9124 (14)	0.6578 (13)	0.061 (7)
C2a	0.3712 (12)	0.7196 (11)	0.5035 (10)	0.036 (5)
O2a'	0.4207 (9)	0.6751 (8)	0.5767 (7)	0.042 (4)
N3a	0.2975 (9)	0.6540 (8)	0.3910 (8)	0.033 (4)
C4a	0.2448 (12)	0.7079 (11)	0.3084 (11)	0.037 (5)
O4a'	0.1764 (9)	0.6463 (8)	0.1998 (7)	0.045 (4)
C5a	0.2661 (14)	0.8317 (12)	0.3420 (12)	0.048 (6)
C6a	0.3333 (15)	0.8963 (13)	0.4529 (12)	0.049 (7)
N1b	-0.0015 (11)	0.3416 (11)	0.4644 (9)	0.046 (5)
C1b'	0.0101 (17)	0.2834 (15)	0.5567 (15)	0.063 (8)
C2b	0.1215 (13)	0.3858 (12)	0.4586 (12)	0.045 (6)
O2b'	0.2288 (9)	0.3806 (8)	0.5277 (8)	0.046 (4)
N3b	0.1079 (10)	0.4267 (9)	0.3646 (8)	0.034 (4)
C4b	-0.0131 (13)	0.4288 (13)	0.2894 (11)	0.043 (6)
O4b'	-0.0269 (8)	0.4645 (8)	0.2032 (7)	0.044 (4)
C5b	-0.1360 (14)	0.3899 (15)	0.3007 (12)	0.054 (7)
C6b	-0.1240 (13)	0.3470 (14)	0.3879 (13)	0.054 (7)
N30	0.3542 (16)	0.1875 (13)	0.6236 (18)	0.076 (9)
O30	0.3983 (14)	0.1959 (11)	0.5498 (14)	0.093 (9)
O31	0.2405 (15)	0.1081 (13)	0.5850 (15)	0.110 (10)
O32	0.4181 (21)	0.2552 (14)	0.7194 (15)	0.131 (11)
N40	0.4223 (16)	0.2396 (13)	0.1104 (12)	0.061 (7)
O40	0.4734 (16)	0.3480 (13)	0.1517 (11)	0.094 (8)
O41	0.3201 (13)	0.1907 (12)	0.1167 (11)	0.090 (7)
O42	0.4734 (23)	0.1825 (17)	0.0626 (21)	0.172 (19)
O50	0.0802 (23)	0.1103 (14)	0.3297 (17)	0.179 (16)
O51	0.1816 (28)	0.0134 (26)	0.7390 (25)	0.217 (26)
O52	0.3523 (39)	0.9596 (33)	0.9055 (30)	0.281 (34)

The magnetic moment of a HNO_3 -containing sample of **2**, determined at room temperature, was $\mu_{\text{eff}} = 1.70 \mu_{\text{B}}$, consistent with one unpaired spin per Pt_4 . The EPR spectrum of **2a** (solid state) is rather similar to that of the α -pyridone blue, with an intense g_{\perp} signal in the first derivative spectrum at 2.291 and a weaker g_{\parallel} signal at 1.997 (cf. supplementary material), suggesting a similar delocalization of the unpaired spin over all four Pt centers as in the α -pyridone blue. A hyperfine splitting of the signals was not observed. The EPR spectrum of **2c** was slightly different from that of **2a** in that two weak additional features on either side of the g_{\perp} signal were observed, which could arise from either a reduction in axial symmetry in **2c**, a poorly resolved hyperfine splitting,¹⁴ or an admixture of a species other than **2a**.

The visible spectra of $\{[(\text{NH}_3)_2\text{Pt}(\text{1-MeU})_2\text{Pt}(\text{bpy})]_2\}(\text{NO}_3)_5 \cdot m\text{HNO}_3 \cdot n\text{H}_2\text{O}$, prepared via either of the two routes, show two absorption maxima at 800 and 568 nm (Figure 1). Extinction coefficients determined for nine different samples in 1.4 N HNO_3 were between 22 900 and 28 500 $\text{M}^{-1} \text{cm}^{-1}$ (800 nm) and between 9800 and 12 100 $\text{M}^{-1} \text{cm}^{-1}$ (568 nm), respectively. The observed variations in ϵ values (cf. discrepancies in ϵ values observed for $\{[(\text{NH}_3)_2\text{Pt}(\text{1-MeU})_2\text{Pt}(\text{NH}_3)_2]_2\}(\text{NO}_3)_5 \cdot 5\text{H}_2\text{O}$ ¹⁵) appear to be, at least in part, due to the concentration dependence of ϵ (Table

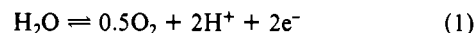
**Figure 1.** Visible spectrum of **2** in 1.4 N HNO_3 . Dissolving **2** in H_2O leads to rapid decomposition of **2**. The dashed curve shows the absorption spectrum of **2** in H_2O after 24 h. It is identical with the spectrum of **1**.**Table IV.** Concentration Dependence of ϵ of **2**^a

c, M	$\epsilon_{800}, \text{M}^{-1} \text{cm}^{-1}$	$\epsilon_{568}, \text{M}^{-1} \text{cm}^{-1}$
1.841×10^{-4}	22 920 (100%)	9800 (100%)
3.682×10^{-5}	22 542 (98%)	8550 (92%)
1.841×10^{-5}	21 180 (87%)	6520 (67%)

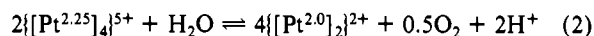
^a Recorded in 1.4 M HNO_3 solution.

IV). As expected for a system comprising a dimer of dimers, the intensities of intervalence absorptions are concentration dependent. As one goes from a concentration of 1.84×10^{-4} to 1.84×10^{-5} M, the ϵ values decrease by ca. 13% (800 nm) and ca. 30% (570 nm), for example.

UV-vis measurements of **2** in different solvents show a reasonable stability of **2** in 1.4 N HNO_3 only. In this solvent, the visible spectrum virtually does not change within 1 day at 22 °C, whereas in more dilute acid and especially in water, the absorptions in the visible part of the spectrum decrease and/or eventually disappear within hours, leaving a slightly yellow solution with an absorbing species at $\lambda = 420$ nm (isosbestic point at 456 nm). The diplatinum(II) complex **1** absorbs at the very same wavelength, and the ^1H NMR results (vide infra) are consistent with formation of **1**. This process is accompanied by a drop in pH (see below). We suggest that, as with $\{[(\text{bpy})\text{Pt}(\text{1-MeU})_2\text{Pt}(\text{bpy})]_2\}^{5+}$, for which such a process has unambiguously been proven by mass spectroscopy and the use of ^{18}O enriched water,¹⁶ water is oxidized according to

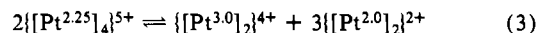


consistent with the following reaction:

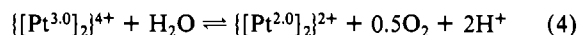


Water oxidation has also been reported by Matsumoto et al both for tetraplatinum(3.0)¹⁷ and tetraplatinum(2.5)^{3c} complexes containing bridging α -pyrrolidone ligands. Depending on conditions (solid state, solution, pH), reaction products are Pt(2.5), Pt(2.25), or Pt(2.0) species.

On the basis of these results, we considered the possibility that a diplatinum(3.0) species, generated from Pt(2.25) in a disproportionation process



might act as the ultimate oxidant:



In that case, reaction 4 should be very fast. At present we do not have experimental evidence for this pathway, but the more positive

(14) Cf. a similar spectrum reported (Figure 7): Arrizabalaga P.; Castan, P.; Geoffroy, M.; Laurent, J.-P. *Inorg. Chem.* **1985**, *24*, 3656.

(15) Cf. refs 17, 18 in: Lippert, B.; Schöllhorn, H.; Thewalt, U. *Inorg. Chem.* **1987**, *26*, 1736.

(16) Micklitz, W. Ph.D. Thesis, Technical University Munich, 1987.

(17) Matsumoto, K.; Watanabe, T. *J. Am. Chem. Soc.* **1986**, *108*, 1308.

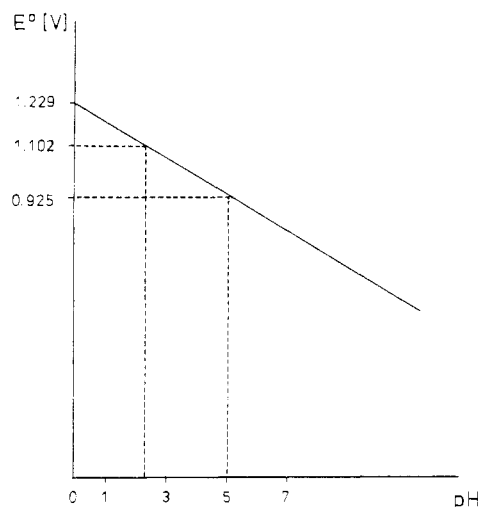


Figure 2. pH dependence of E° for water oxidation.

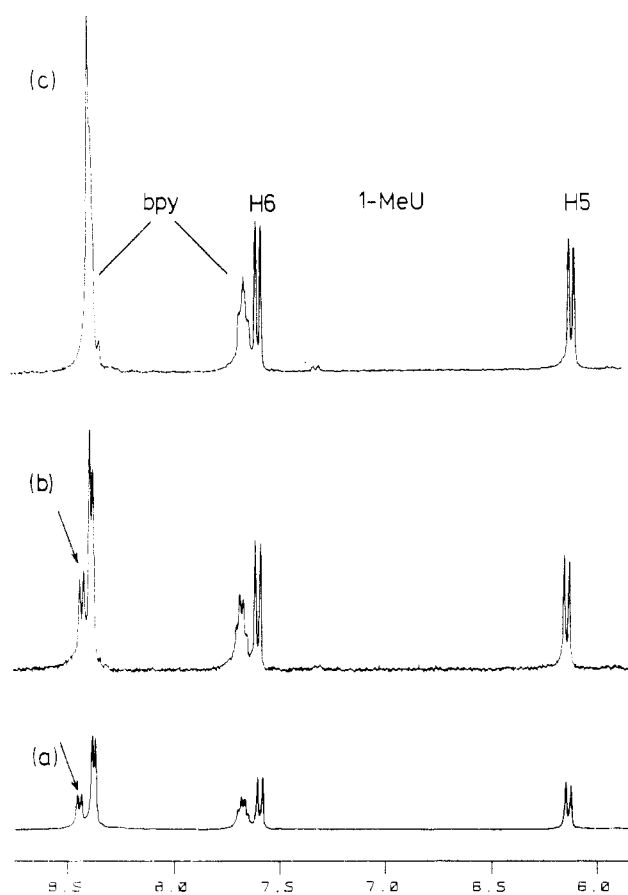


Figure 3. Low-field portion of 300-MHz ^1H NMR spectra of **1** (**1***): (a) 0.7 mg/0.65 mL of D_2O , pD = 5.1; (b) 1.4 mg/0.65 mL of D_2O , pD = 4.9; (c) saturated solution, pD = 5.3. Note the upfield shift of the bpy resonance at lowest field (spectrum a) with increasing concentration.

redox potential of the Pt(3.0)/Pt(2.0) couple as compared to the Pt(2.25)/Pt(2.0) couple (1102 and 925 mV vs SHE, respectively)⁷ and the pH dependence of the water oxidation process (Figure 2 and eq 5) would make it reasonable. **2** indeed already loses its

$$E^\circ = 1.229 - 0.059 \text{ pH} \quad (5)$$

color at $\text{pH} \approx 2$, whereas water might be expected to undergo oxidation at $\text{pH} \geq 5$ only if Pt(2.25) were the oxidant (see, however, the next paragraph).

^1H NMR Spectra. (i) **Acidic Medium.** Spontaneous reduction of **2** to **1*** also takes place in D_2O . As judged from ^1H NMR spectra, paramagnetic **2** (2 mg/mL, initial pD = 3.0), which has

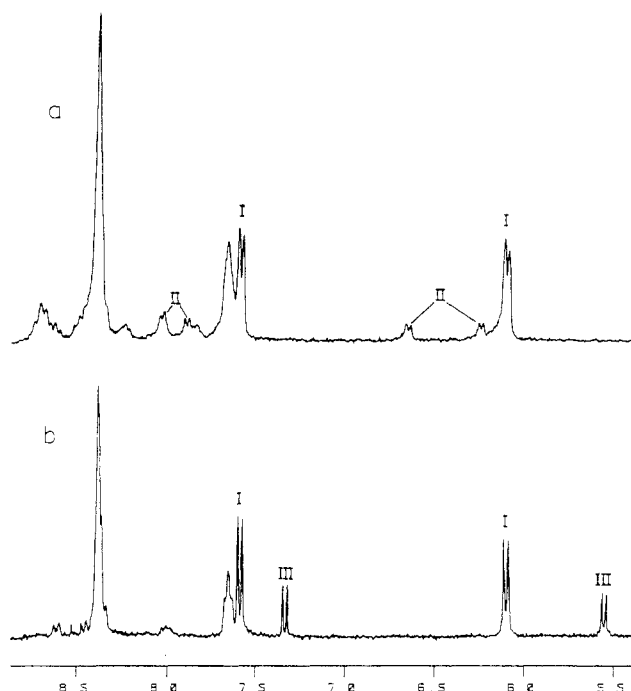


Figure 4. ^1H NMR spectra (D_2O , aromatic region only) of **2d**: (a) immediately after addition of NaOD to give pD = 8.7; (b) after 1 day at 20 $^\circ\text{C}$ (pD dropped to 5). Resonances I correspond to H5, H6 (1-MeU) of **1**, resonances II are assigned to a diplatinum(3.0) species (cf. text) having two nonequivalent 1-MeU ligands, and resonances III are due to *cis*-(NH_3)₂Pt(1-MeU)₂. Unmarked resonances are due to bpy-containing species (**1**, diplatinum(3.0) complex, decomposition product).

an almost featureless spectrum, is converted within 24 h at 40 $^\circ\text{C}$ to the diamagnetic complex **1***, which displays sharp resonances again. More concentrated solutions of **2** (e.g. 18 mg/1 mL) take a considerably longer time to fully convert to **1***. The reaction **2** \rightarrow **1*** appears to be remarkably clean with no major side products and especially no intermediates (e.g. $[\text{Pt}^{3.0}]_2$) observable in the ^1H NMR spectrum. Originally we were puzzled by the fact that there were slight differences in the positions of bpy resonances of **1**, dissolved in D_2O , and of **1*** generated via reduction of **2** in D_2O at identical pD values. We subsequently became aware of the fact that the bpy resonances are concentration dependent (Figure 3). Thus the resonance at lowest field shifts upfield as the concentration of **1** increases, which is indicative of intermolecular association of **1** via bpy stacking in solution. To our knowledge, this is the first definite proof that diplatinum(II) compounds form dimer of dimers in aqueous solution (cf. also X-ray results).

(ii) **Slightly Alkaline Medium.** Addition of NaOD to a solution of **2** in D_2O up to pD = 8.7, which corresponds approximately to the end point of the second titration step of **2** with OH^- (vide infra), instantaneously generates a spectrum with three sets of 1-MeU resonances of relative intensities close to 1:1:6 (Figure 4a). The major set (I) (δ (ppm): H6, 7.58; H5, 6.09; CH_3 , 3.42) corresponds to **1**. The two minor sets (II) (δ (ppm): H6, 8.00 and 7.86; H5, 6.63 and 6.22; CH_3 , 3.49 and 3.38) disappear within hours, during which the pD drops to 5. Within 1 day, new resonances due to *cis*-(NH_3)₂Pt(1-MeU)₂ are formed (III, Figure 4b). It appears that resonances III initially grow at the expense of II and later also at the expense of I. Signals II are tentatively assigned to a diplatinum(3.0) complex containing two nonequivalent 1-MeU ligands for the following reasons. First, relative intensities of both sets appear to be 1:1 at any time of the existence of this compound. The accidental existence of two different compounds of equal concentrations is considered unlikely. Second, chemical shifts of II do not match any of the known mono- or dinuclear 1-MeU complexes of *cis*- $\text{A}_2\text{Pt}^{\text{II}}$ ($\text{A}_2 = \text{bpy}$ or $(\text{NH}_3)_2$) containing monodentate (N3) or bridging (N3, O4) 1-MeU rings. However, a diplatinum(3.0) complex generated from **1** with concentrated DNO_3 displays resonances (δ (ppm): H6, 7.85; H5,

Scheme I

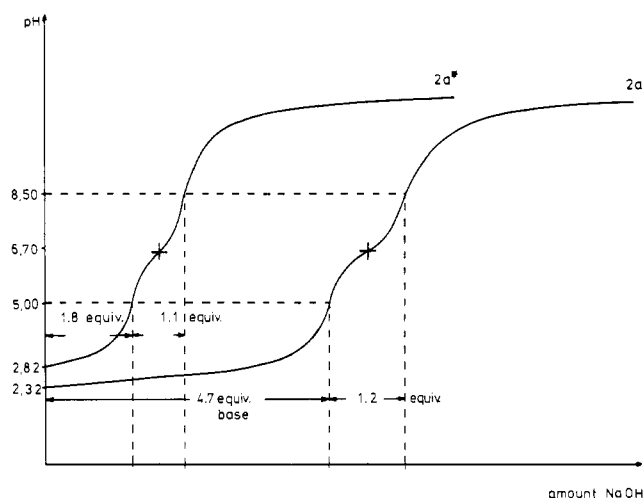
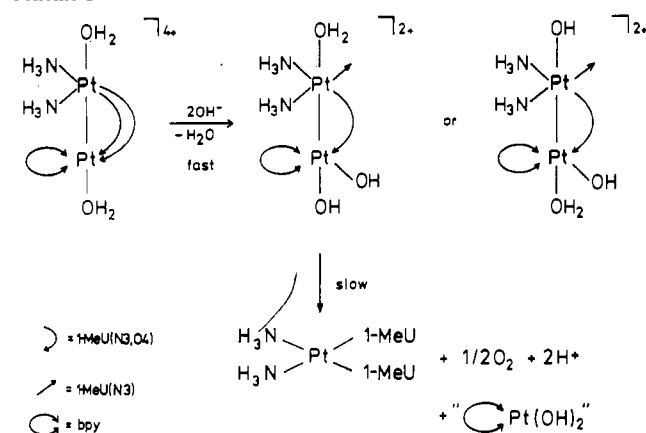


Figure 5. NaOH titration curves of **2** and **2a***. Amounts of compounds used were *not* equimolar.

6.62; CH₃, 3.53) close to those of one of the two sets of II. Third, relative intensities of I and II are consistent with an initial disproportionation reaction (eq 3), which is followed by a rapid modification of the diplatinum(3.0) complex. A feasible description of this latter process and the subsequent reaction that eventually leads to *cis*-(NH₃)₂Pt(1-MeU)₂ and a (bpy)Pt(2.0)¹⁸ species is given in Scheme I.

Potentiometric Titration of 2. Figure 5 depicts titration curves (with NaOH) of two samples of **2** that, according to elemental analysis (based on the C:N ratio, assuming a dimer-of-dimer structure with Pt(2.25) average oxidation state), contain different amounts of HNO₃: **2a** (4.6 HNO₃) and **2a*** (1.4 HNO₃). Traces for **2a** and **2a*** represent typical titration curves for mixtures containing a strong and a weak acid. As expected, the pH of a solution of **2a** (2.32) is lower than that of **2a*** (2.82). Both samples are blue-violet. The first inflection points, reached at pH = 5 (samples now red-purple) are measures for the neutralization of the strong acid HNO₃ in **2a** and **2a***. The NaOH consumed at these points amounts to 4.7 and 1.8 equiv of HNO₃ for **2a** and **2a***, respectively. These values agree reasonably well with those deduced from elemental analysis data reported in Table I.

The second neutralization steps of **2a** and **2a*** are complete at pH = 8.5–9 (samples yellow) and require ca. 1 equiv of NaOH/2. From the pH at half-titration, a pK_a of ca. 6.7 is deduced.

Samples of freshly dissolved **2d** show qualitatively similar titration curves, except that the amount of strong acid is 0.3–0.5 equiv only. The second titration step again amounts to ca. 1 equiv of NaOH (Figure 6, trace i). According to elemental analysis,

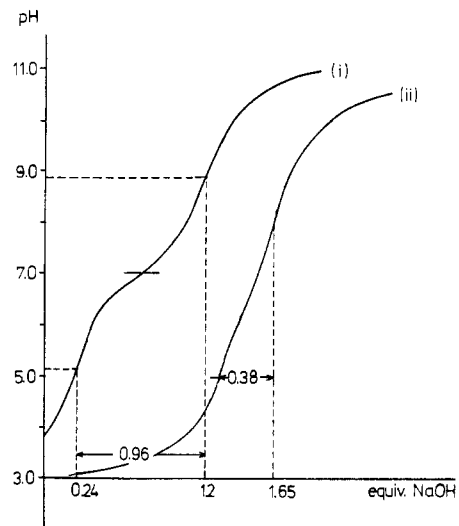
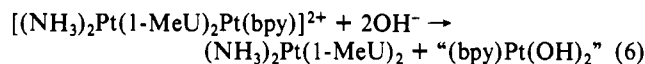


Figure 6. NaOH titration curves of **2d**: (i) immediately after dissolving in H₂O; (ii) 5 days after dissolving in H₂O (kept at 30 °C). Titrations were carried out with identical concentrations of compounds.

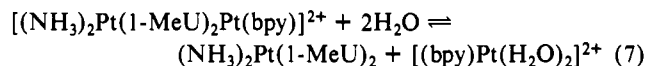
2d should not contain any extra HNO₃. However, 0.3–0.5 equiv of HNO₃/**2d** would mean a 1% (by weight) “impurity” of HNO₃ in **2d**, which is not unrealistic considering isolation of **2d** from HNO₃ solutions of pH ≤ 1 (cf. Experimental Section).

As to the origin of the second titration step (pH 5–8, pK_{app} ≈ 6.7), we can exclude the possibility that it is associated with the diplatinum(2.0) complex **1** formed according to eq 3. **1** does not (at pH 8¹⁹) consume any OH⁻ within the time of the titration experiment, although in a slow process (many hours), OH⁻ is used up to cleave the Pt–O4 bonds:



Results of the ¹H NMR experiments (cf. part ii, above) suggest that OH⁻ consumption is associated with a modification of a diplatinum(3.0) species (cf. Scheme I). The amount of OH⁻ consumed (1 equiv/tetramer) and the apparent pK_a value (assumed to be the mean of two similar pK_a values) is not inconsistent with Pt(III)–OH₂ entities being involved.²⁰

The titration curve of aged **2d** (Figure 6, trace ii) displays a first end point (pH ≈ 5) after addition of 1.27 equiv of NaOH and a second one (pH ≈ 8) after an additional 0.38 equiv of NaOH. The first end point must be due to the titration of strong acid already present in sample **2d** plus the acidic protons generated according to eq 4. The additional consumption of base (0.38 equiv) is assigned to deprotonation of decay products of **1**, most probably [(bpy)Pt(H₂O)₂]²⁺. We conclude this from the following experiment: An aqueous solution of **1** was brought to pH 3.5 by addition of HNO₃, divided in exactly two parts, and titrated with NaOH immediately after sample preparation and after 2 days at 30 °C. The aged sample displayed a distinctly higher consumption of base and two steps in the titration curve very similar to trace ii in Figure 6. We suggest that in moderately acidic solution, the dinuclear structure of **1** is lost in part, viz.



and that NaOH is consumed to neutralize the moderately acidic protons of the [(bpy)Pt(H₂O)₂]²⁺ species.

Description of 1. Figure 7 gives a view of the molecular cation of *cis*-[(NH₃)₂Pt(1-MeU)₂Pt(bpy)](NO₃)₂·3H₂O, **1***, obtained from **2** in water. According to spectroscopic (IR, ¹H NMR, UV/vis), crystallographic (cell constants), and elemental analysis

(18) According to ¹H NMR spectroscopy, the bpy-containing species is not (bpy)Pt(OH)₂ but rather a species possibly identical with **4**: Wimmer, S.; Castan, P.; Wimmer, F. L.; Johnson, N. P. *Inorg. Chim. Acta* **1988**, *142*, 13.

(19) In strongly alkaline medium (pD = 12–13), **1** is rapidly altered, however.

(20) Schöllhorn, H.; Eisenmann, P.; Thewalt, U.; Lippert, B. *Inorg. Chem.* **1986**, *25*, 3384.

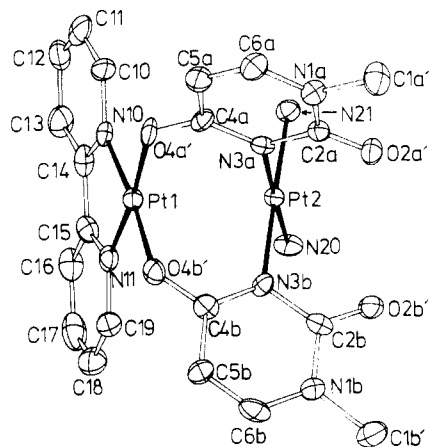


Figure 7. ORTEP drawing of the molecular cation $cis-[(NH_3)_2Pt(1-MeU)_2Pt(bpy)]^{2+}$ (head-head) (**1***).

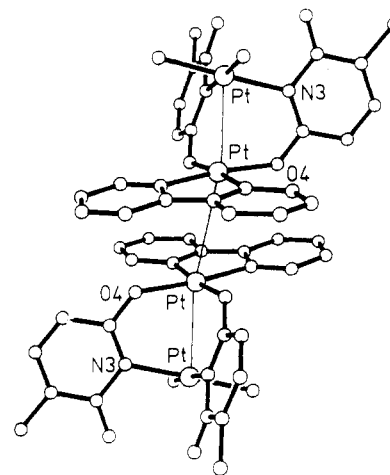


Figure 8. Cation stacking in **1***.

Table V. Interatomic Distances (Å) and Angles (deg) for **1***

Pt1–Pt2	2.929 (1)	C18–C19	1.39 (2)
Pt1–N10	2.00 (1)	C19–N11	1.36 (2)
Pt1–N11	1.99 (1)	N1a–C1a'	1.48 (2)
Pt1–O4a'	2.01 (1)	N1a–C2a	1.40 (2)
Pt1–O4b'	2.05 (1)	C2a–O2a'	1.21 (1)
Pt2–N20	2.06 (1)	C2a–N3a	1.35 (1)
Pt2–N21	2.07 (1)	N3a–C4a	1.38 (1)
Pt2–N3a	2.06 (1)	C4a–O4a'	1.30 (1)
Pt2–N3b	2.05 (1)	C4a–C5a	1.40 (2)
N10–C10	1.34 (2)	C5a–C6a	1.33 (2)
C10–C11	1.38 (2)	C6a–N1a	1.36 (2)
C11–C12	1.33 (3)	N1b–C1b'	1.51 (2)
C12–C13	1.42 (2)	N1b–C2b	1.40 (2)
C13–C14	1.43 (2)	C2b–O2b'	1.21 (2)
C14–N10	1.34 (2)	C2b–N3b	1.41 (2)
C14–C15	1.45 (2)	N3b–C4b	1.33 (2)
N11–C15	1.35 (2)	C4b–O4b'	1.28 (2)
C15–C16	1.40 (2)	C4b–C5b	1.43 (2)
C16–C17	1.41 (2)	C5b–C6b	1.34 (2)
C17–C18	1.37 (2)	C6b–N1b	1.37 (2)
Pt2–Pt1–N10	106.6 (3)	Pt1–Pt2–N20	99.4 (3)
Pt2–Pt1–N11	105.3 (3)	Pt1–Pt2–N21	99.6 (3)
Pt2–Pt1–O4a'	80.1 (2)	Pt1–Pt2–N3a	82.3 (3)
Pt2–Pt1–O4b'	78.5 (2)	Pt1–Pt2–N3b	81.9 (3)
N10–Pt1–N11	81.0 (5)	N20–Pt2–N21	88.6 (4)
N10–Pt1–O4a'	95.2 (4)	N20–Pt2–N3a	178.1 (4)
N10–Pt1–O4b'	174.3 (4)	N20–Pt2–N3b	89.4 (4)
N11–Pt1–O4a'	174.1 (4)	N21–Pt2–N3a	90.1 (4)
N11–Pt1–O4b'	95.3 (4)	N21–Pt2–N3b	178.0 (4)
O4a'–Pt1–O4b'	88.1 (4)	N3a–Pt1–N3b	91.5 (4)

data, **1*** is identical with the starting compound **1**. Selected interatomic distances and angles of the cation are given in Table V. The $cis-(NH_3)_2Pt^{II}$ entity binds to the N3 positions of two 1-MeU rings, whereas the $(bpy)Pt^{II}$ is coordinated to the O4 sites of the two rings. The overall feature of the cation thus resembles that of a series of related diplatinum(II) complexes with 1-MeU and 1-MeT (1-methylthyminato) ligands in head-head arrangement.²¹ The Pt...Pt distance within the cation (2.929 (1) Å) and the tilting of the two Pt planes (30.4°) are very similar to those in the bis(diammineplatinum(II)) analogues.²¹ The twist angle about the Pt–Pt vector (e.g. N11–Pt1–Pt2–N20) is 10.2°, smaller than that in most previously studied cases. There are no unusual details of the structure that have not been observed in the related compounds. Thus, both Pt atoms are directed toward each other, deviations from the respective coordination planes being 0.08 Å

Table VI. Close Contacts (Å, deg) in **1***^a

N20–O41	2.95	Pt2–N20–O41	118
N20–O50	2.93	Pt2–N20–O50	122
N21–O40	2.95	Pt2–N21–O40	114
O30–O50	3.35	N30–O30–O50	94
O31–O51	2.78	N30–O31–O51	118
O42–O52 ¹	2.70	N40–O42–O52 ¹	128
O51–O52 ²	2.59		
O50–O51 ³	2.66		
N20–O2a' ⁴	2.93	Pt2–N20–O2a' ⁴	102
N21–O2a' ⁴	3.04	Pt2–N21–O2a' ⁴	98
N21–O2b' ⁴	2.92	Pt2–N21–O2b' ⁴	146
N21–O30 ⁴	3.16	Pt2–N21–O30 ⁴	107
N21–O32 ⁴	3.13	Pt2–N21–O32 ⁴	125
O42–O52 ⁴	2.80	N40–O42–O52 ⁴	143
O52–O52 ⁵	3.04		

^aSymmetry operations: (1) $x, -1 + y, -1 + z$; (2) $x, -1 + y, z$; (3) $-x, -y, 1 - z$; (4) $1 - x, 1 - y, 1 - z$; (5) $1 - x, 2 - y, 2 - z$.

(Pt1) and 0.02 Å (Pt2), respectively, and the O4-bound Pt1 deviates quite substantially from the 1-MeU planes (–0.79 Å from plane *b*; –0.40 Å from plane *a*). With Pt2, this effect is much smaller, +0.11 Å from ring *a* and –0.11 Å from ring *b*. For a complete list of planes, deviations of atoms from best planes, and dihedral angles see the supplementary material.

Pairs of centrosymmetric cations are arranged such that $(bpy)Pt1(O4)_2$ planes stack on top of each other, giving rise to an intermolecular Pt1...Pt1' separation of 3.489 Å and an angle of 165.7° for Pt2–Pt1–Pt1' (Figure 8). In addition, pairs of cations are connected through hydrogen bonding between NH_3 groups of Pt2 (N20, N21) and the exocyclic O2 sites of an adjacent cation (type I²¹), leading to a Pt2...Pt2' separation of 4.627 Å and a Pt1–Pt2–Pt2' angle of 155.8°. As a result, infinite zigzag chains of Pt₂ units having three different Pt–Pt distances of 2.929, 3.489, and 4.627 Å are formed, a pattern very similar to that observed with $cis-[(NH_3)_2Pt(1-MeU)_2Pd(en)]^{2+}$.⁷ Nitrate anions and water molecules are located in channels between the Pt₂ strands and are connected with the latter via hydrogen bonds involving the NH_3 ligands. Additional hydrogen bonds are observed between NO_3^- and H_2O as well as between H_2O molecules (Table VI).

Summary

A Pt(2.25)–1-methyluracil blue is described that contains different amine ligands (*bpy*, $(NH_3)_2$) bound to Pt. Isolation from strongly HNO_3 acidic solution leads to incorporation of HNO_3 in stoichiometric amounts (**2a**, **2b**) or as an "impurity" (**2d**). HNO_3 has been analyzed by using elemental analysis and/or titration with base. A complication arises from the fact that the Pt(2.25) blue, when dissolved in water, generates additional protons. In the initial step, these protons are weakly acidic ($pK_a(av) = 6.7$) and are believed to be due to aqua ligands in a diplatinum(III) complex. In a slow secondary process, the di-

- (21) (a) Schöllhorn, H.; Thewalt, U.; Lippert, B. *Inorg. Chim. Acta* **1984**, *93*, 19 and references cited therein. (b) Micklitz, W.; Sheldrick, W. S.; Lippert, B. *Inorg. Chem.* **1990**, *29*, 211. (c) Lippert, B.; Neugebauer, D.; Raudaschl, G. *Inorg. Chim. Acta* **1983**, *78*, 161.
 (22) (a) Hollis, L. S.; Lippard, S. J. *J. Am. Chem. Soc.* **1983**, *105*, 3494; *Inorg. Chem.* **1983**, *22*, 2600. (b) Laurent, J.-P.; Lepage, P.; Dahan, F. *J. Am. Chem. Soc.* **1982**, *104*, 7335.

platinum(III) species disappears and strongly acidic protons are generated, formed in a redox process involving oxidation of water.

Acknowledgment. We acknowledge, with thanks, financial support by the Deutsche Forschungsgemeinschaft, the Fonds der Chemischen Industrie, and Degussa (loan of K_2PtCl_4).

Notes

Contribution from the Department of Chemistry,
National Tsing Hua University,
Hsinchu, Taiwan 30043, Republic of China

Homogeneous Catalytic Reduction of Nitric Oxide by Olefin in the Presence of Palladium(II) Chloride

C. H. Cheng* and K. S. Sun

Received September 20, 1989

The catalytic reduction of NO by CO, NH_3 , H_2 , or hydrocarbons over a heterogeneous system¹ has been investigated in an effort to find suitable ways to remove these pollutants in automobile emission. Similar attempts to reduce NO by using homogeneous catalysts also led to the development of several successful catalyst systems. To date, however, only the reduction of NO by CO^{2-8} and by NH_3^9 has been reported. In the present paper, we describe the reduction of NO by olefin catalyzed by a soluble $PdCl_2$ system (reaction 1) under mild conditions. This



catalytic reaction is the first one using hydrocarbons for NO removal homogeneously. In addition, it also appears to be a useful method for making organic carbonyl compounds from olefins.

In choosing an appropriate catalyst system for reaction 1, we were attracted to the $PdCl_2-CuCl_2$ system in view of the fact that $PdCl_2$ is known to oxidize olefin to ketone or aldehyde¹⁰ and the $PdCl_2-CuCl_2$ system is found to catalyze the reduction of NO by CO .⁵ A simple catalyst system was obtained consisting of $PdCl_2$ and $CuCl_2$ dissolved in water. The catalysis of reaction 1 takes place at ambient temperature under an initial NO pressure of

Supplementary Material Available: Tables of positional parameters and anisotropic temperature factors for **1*** and equations of planes, deviations of atoms, and dihedral angles for **1*** and figures showing EPR spectra of **2a** and **2c** (4 pages); a listing of observed and calculated structure factors (20 pages). Ordering information is given on any current masthead page.

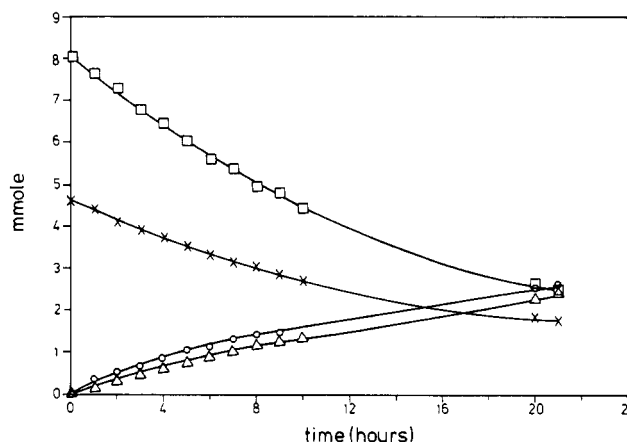


Figure 1. Change of compositions as a function of time for the catalytic reduction of NO by ethylene using the $PdCl_2-CuCl_2-H_2O$ system at 19 °C: nitric oxide (\square); ethylene (\times); nitrous oxide (Δ); acetaldehyde (O).

less than 1 atm. While quantitative analysis of each component was performed on gas chromatographs, the identities of the organic products were verified by comparing their IR 1H NMR, and mass spectra with those of authentic samples. The quantitative data of several reaction runs are summarized in Table I, and changes of reactants and products vs time for the reaction of NO with ethylene are displayed in Figure 1.

The stoichiometry for the catalysis of reaction 1 by the $PdCl_2-CuCl_2-H_2O$ system is indicated by the relative ratio of NO and olefin consumed and N_2O and carbonyl compound produced, shown in Table I. The rate of catalysis at ambient temperature corresponds to 0.384, 0.255, 0.298, and 0.190 (turnovers/h)/palladium ion on the basis of N_2O produced for ethylene, propylene, 1-butene, 1-hexene, respectively (runs I-IV). These terminal olefins were converted exclusively to the corresponding 2-ketones. No other organic product was detected by GC. Notable here is that the reaction NO with an internal olefin such as cyclohexene is extremely slow under reaction conditions similar to those for terminal olefin. In the absence of $CuCl_2$, $PdCl_2$ in a mixture of DMSO and water (9:1 v/v) is also effective for the catalysis of reaction 1. No palladium precipitation was observed under the conditions used. Quantitative data of the reactions catalyzed by the system are shown in Table I (runs V-VIII). Surprisingly, other solvent mixtures such as acetonitrile-water and DMF-water exhibit much smaller activities for the catalysis (runs IX and X).

During the catalysis of reaction 1 by the $PdCl_2-CuCl_2-H_2O$ system, the reaction solution exhibited an absorption at 425 nm in the UV-vis spectrum. This band is close to the absorption at 421 nm for a pure $PdCl_2$ solution.¹¹ There is no evidence for the coordination of olefin or NO to the palladium. To understand further the features of catalysis by $PdCl_2-CuCl_2-H_2O$, several control experiments were carried out, leading to the following observations. (i) No catalysis takes place in the absence of $PdCl_2$. (ii) A reaction solution with 0.59 M LiCl present has only 82% of the catalytic activity in its absence. (iii) The presence of 0.55

- (1) Reviews: (a) Shelef, M. *Catal. Rev.—Sci. Eng.* **1975**, *11*, 1. (b) McCleverty, J. A. *Chem. Rev.* **1979**, *79*, 53. (c) Harrison, B.; Wyatt, M.; Gough, K. G. In *Catalysis (Specialist Periodical Reports)*; Bond, G. C.; Webb, G., Eds.; Royal Society of Chemistry: London, 1982; Vol. 5, p 127. (d) Egelhoff, W. F., Jr. In *The Chemical Physics of Solid Surfaces and Heterogeneous Catalysis*; King, D. A.; Woodruff, D. P., Eds.; Elsevier: New York, 1982; p 397.
- (2) (a) Johnson, B. F. G.; Bhaduri, S. *J. Chem. Soc., Chem. Commun.* **1973**, 650. (b) Bhaduri, S.; Johnson, B. F. G.; Savory, C. J.; Segal, J. A.; Walter, R. H. *Ibid.* **1974**, 809. (c) Bhaduri, S.; Johnson, B. F. G. *Transition Met. Chem.* **1978**, *3*, 156.
- (3) (a) Haymore, B. L.; Ibers, J. A. *J. Am. Chem. Soc.* **1974**, *96*, 3325. (b) Kaduk, J. A.; Tulip, T. H.; Budge, J. R.; Ibers, J. A. *J. Mol. Catal.* **1981**, *12*, 239.
- (4) (a) Reed, J.; Eisenberg, R. *Science* **1974**, *184*, 568. (b) Meyer, C. D.; Eisenberg, R. *J. Am. Chem. Soc.* **1976**, *98*, 1364.
- (5) (a) Kubota, M.; Evans, K. J.; Koerntgen, C. A.; Marsters, J. C., Jr. *J. Am. Chem. Soc.* **1978**, *100*, 342. (b) Kubota, M.; Evans, K. J.; Koerntgen, C. A.; Marsters, J. C., Jr. *J. Mol. Catal.* **1980**, *7*, 481.
- (6) Chin, C. S.; Sennett, M. S.; Wier, P. J.; Vaska, L. *Inorg. Chim. Acta* **1978**, *31*, L443.
- (7) Dorfman, Y. A.; Emel'yanova, V. S.; Zhusupbekov, B. O. *Kinet. Katal.* **1981**, *22*, 375.
- (8) (a) Fang, W. P.; Cheng, C. H. *J. Chem. Soc., Chem. Commun.* **1986**, 503. (b) Sun, K. S.; Cheng, C. H. *J. Am. Chem. Soc.* **1988**, *110*, 6744.
- (9) Naito, S.; Tamaru, K. *J. Chem. Soc., Faraday Trans. 1* **1982**, *78*, 735.
- (10) (a) Smidt, J.; Hafner, W.; Jira, R.; Sedlmeier, J.; Sieber, R.; Ruttinger, R.; Kojer, H. *Angew. Chem.* **1959**, *71*, 176. (b) Smidt, J.; Hafner, W.; Jira, R.; Sieber, R.; Sedlmeier, J.; Sabel, A. *Angew. Chem., Int. Ed. Engl.* **1962**, *1*, 80. (c) Jira, R.; Sedlmeier, J.; Smidt, J. *Ann. Chem.* **1966**, *693*, 99.

(11) Sundaram, A. K.; Sandell, E. G. *J. Am. Chem. Soc.* **1955**, *77*, 855.